# Research on Optimization of Radome Based on Phased Array Radar-Seeker

Huang Feng-Sheng(✉), Chen Ming, and Wang Kai

38th Research Institute, China Electronic Technology Corporation, Hefei 230031, China

**Abstract.** As protection of radar-seeker, the shape and material of the radome may have great influence on the radar antenna beam. In this paper, we provided the modeling and simulation of antenna and radome and analyzed the influence of antenna beam with radome. With the method of intrinsic extraction adopted, we the optimization of the antenna beam with radome by adjusting the phase compensation realized value of phased array element, and the simulation is provided.

**Keywords:** Compensation · Phased array · Radar-seeker · Radome

## 1 Introduction

With the rapid development of modern military technology, precision-guided weapons have become an effective means of implementing precision strikes. Radar-seeking missiles, as an important branch of precision-guided weapons, occupy an important position in the missile weapon family. Radome is a common device to protect the radar antenna of the seeker, which is located in the head of the missile to avoid the radar antenna being damaged by the harsh external environment. In general, it is both an integral part of the missile body and the radar guidance system [1–10].

After the radome is installed on the missile head, the radome shape, processing accuracy and material consistency will definitely have certain effects on the electrical performance of the radar antenna: the radome wall will cause attenuation to the electromagnetic wave from the antenna, resulting in transmission loss, reflection and refraction to the electromagnetic wave. Thus it has caused the deterioration of the antenna sub-flap; phase insertion and refraction to the electromagnetic wave causing the beam pointing offset. The final cause of the radar wave through the radome when the distortion of radiation pattern of the antenna, including attenuation loss, sub-flap elevation, zero depth drop and pointing offset and other effects. For the seeking missiles, the main characterization is the deterioration of the aiming error and aiming error slope.

## 2 Current Situation and Problems

At present, through the analysis of the radome characteristics and the working principle of the seeker, two types of methods are usually used to compensate the radome error: One is


X. Wang et al. (Eds.): AICON 2021, LNICST 396, pp. 423–432, 2021.
https://doi.org/10.1007/978-3-030-90196-7_36

the "grinding" method, i.e., the compensation method through mechanical processing, i.e., through the small amount of grinding of the radome inner surface local area, to adjust and improve the performance of the radome error slope purpose [1]. The other is the mathematical compensation method [2], i.e., a filter analysis loop or DSP is used in the missile control loop to achieve compensation of the radome error, and a digital compensation circuit is introduced in the seeker to compensate for the targeting line error component. The mechanism of the first compensation method is to reduce the impact on the radar antenna performance index by correcting the radome characteristics. However, the method is limited by the processing and manufacturing accuracy. While for non-axisymmetric shape radome, it is difficult to achieve. In addition, the mechanism of the second compensation method is to compensate the antenna aiming error from the angle measurement result. On the whole, the above two methods are mainly for the seeking seeker, from the aiming error and error slope angle for compensation. In fact, they do not solve the problems of loss, pointing deviation, deformation and reflection caused by the antenna beam through the radome, and can only compensate the angle measurement results. What's more, they cannot compensate the influence of the radome on the radar antenna radiation pattern characteristics (attenuation, sub-flap, zero depth, pointing).

For phased array seeker, the phased array antenna with radomeis should be regarded as a whole, and the radiation characteristics of each channel of the antenna's antenna unit are adjusted by simulation calculation [3]. So it can realize the optimization of antenna radiation pattern compensation after adding the radome. The basic principle of this method is to calculate the antenna unit amplitude phase change before and after radomeing through modeling and simulation, and to achieve the optimal compensation of antenna radiation pattern by compensating the amplitude phase change of each unit. In this work, the compensation algorithm based on eigen-solution extraction is used to calculate the correction code of phased array antenna unit with cover, and the modeling simulation is carried out to verify the effectiveness of the method [10–14].

## 3 Simulation Results and Discussion

### 3.1 Antenna Simulation

First, a phased array antenna with a center frequency of 20 GHz is designed, as shown in Fig. 1. The antenna array is placed on top of a metal backplane with a spacing of 7 mm.

### 3.2 Radome Simulation

The radome is modeled, for the sake of simplification, the processing error and material consistency of the cowl have been ignored here, only the structural shape and the material of different parts are considered. A conical radome with a height of 1 m and a base radius of 0.25 m is designed here, and the cone top angle is 23.8°, as shown in Fig. 3 below. The radomecone top is spherical structure, while the spherical surface is tangent to the cone surface. And the design of the radome has been taken into account the different head cone, sidewall wall thickness and incidence angle, taking into account the electrical

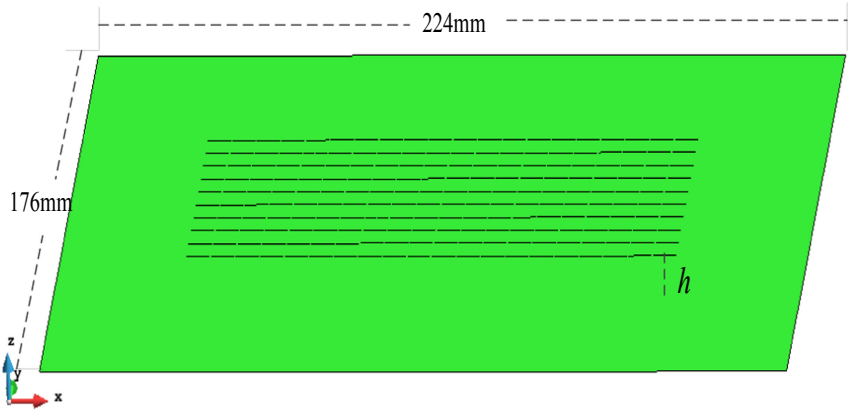


**Fig. 1.** 2D antenna array model.

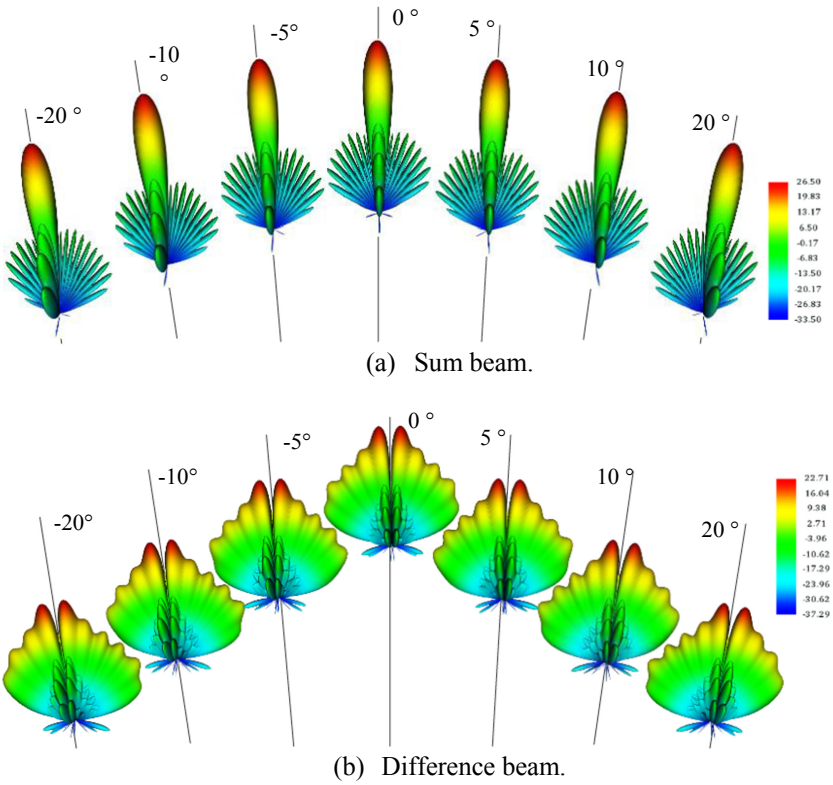


**Fig. 2.** Antenna beam scanning radiation pattern.

properties, mechanical environment requirements. The actual design of the head cone spherical surface and the radomecy cylindrical surface are made of different dielectric materials. Here, the permittivity of dielectric material of head cone spherical surface is 0.005, while the permittivity of dielectric material of cover cylindrical surface is 0.003. Meawhile, the thickness of radome is 12.6 mm, and the antenna installation height is 0.2 m from the cone bottom.

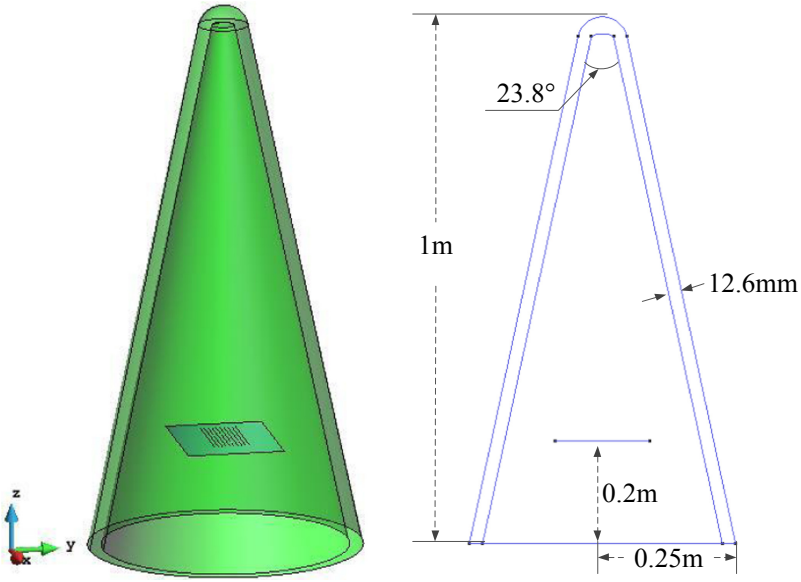


**Fig. 3.** Radome model and structure parameter diagram.

### 3.3 Radiation Simulation

Figure 4 shows the antenna sum and difference radiation pattern after loading the radome with beam pointing at 0°, 5° and 20° for example.

After loading the radome, the gain of both beam and differential beam are reduced, in which the beam gain decreases more obviously the closer to the top of the radome cone. It can be seen that the radome head cone spherical structure relative to the cone structure has a greater impact on the antenna performance such as radiation pattern loss, subflap, differential beam symmetry and aiming.

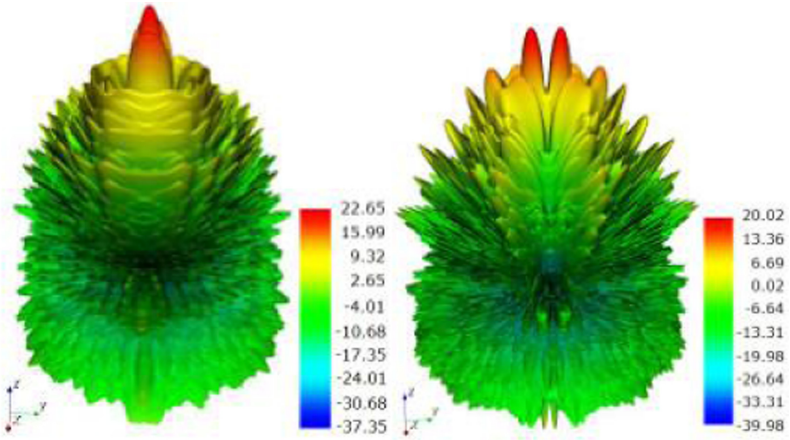


(a) 0° scan, sum and difference beam

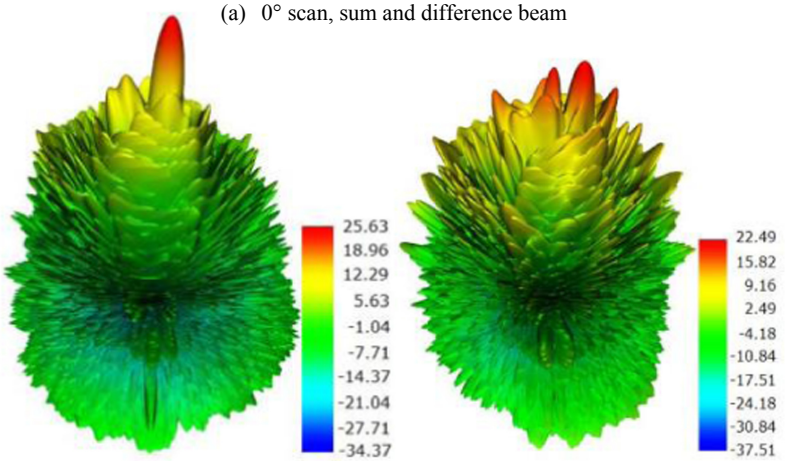


(b) 5°scan, sum and difference beam

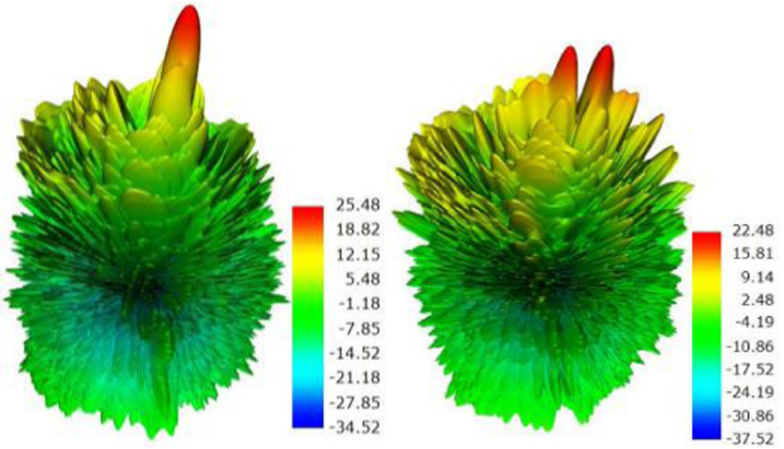


(c) 20°scan, sum and difference beam

**Fig. 4.** Radiation pattern of loaded radome at typical angle.

## 4 Compensation Algorithm Based on Eigen Solution Extraction

The integrated simulation calculation of antenna and radome has been a difficult problem in computational electromagnetics because of its large electrical size and complex structure. Due to the limitation of computational resources, it is difficult to perform accurate calculation by full-wave method in engineering at present. Generally speaking, it is mainly obtained by some approximate methods.

The method of moments (MoM) is a numerical method to transform the integral equation into a linear matrix equation, and the right side of the equation of the matrix equation is the excitation term. When using the MoM to calculate the array antenna, the matrix equation can be written in the following form.

$$\begin{bmatrix} Z_{11} & Z_{12} & \cdots & Z_{1n} \\ Z_{21} & Z_{22} & \cdots & Z_{2n} \\ \vdots & \vdots & \ddots & \vdots \\ Z_{n1} & Z_{n2} & \cdots & Z_{nn} \end{bmatrix} \cdot [I] = \begin{bmatrix} V_1 \\ V_2 \\ \vdots \\ V_n \end{bmatrix} \tag{1}$$

Where the right side of the equation for each unit antenna corresponding to the excitation vector, the matrix equation of the excitation term $V_i$ that is the ith unit of the feed. Calculate the radiation problem under a certain feed state, just give all the unit feed values in turn, and then solve the current coefficient $I$ in Eq. (1) can quickly obtain the radiation characteristics of the antenna. Since the matrix equation is linear, it is also possible to split the excitation vector on the right side into the form of n-units superposition.

$$\begin{bmatrix} Z_{11} & Z_{12} & \cdots & Z_{1n} \\ Z_{21} & Z_{22} & \cdots & Z_{2n} \\ \vdots & \vdots & \ddots & \vdots \\ Z_{n1} & Z_{n2} & \cdots & Z_{nn} \end{bmatrix} \cdot ([I_1] + [I_2] + \cdots + [I_n]) = \left( \begin{bmatrix} V_1 \\ 0 \\ \vdots \\ 0 \end{bmatrix} + \begin{bmatrix} 0 \\ V_2 \\ \vdots \\ 0 \end{bmatrix} + \cdots + \begin{bmatrix} 0 \\ 0 \\ \vdots \\ V_n \end{bmatrix} \right) \tag{2}$$

In Eq. (2), the current coefficient $I_i$ corresponding to the i-th cell feed $V_i$ (it is important to note that the current is not only distributed on the feed cell, but on the whole array). Then the matrix equation can be written for any cell individually excited in the following form.

$$\begin{bmatrix} Z_{11} & Z_{12} & \cdots & Z_{1n} \\ Z_{21} & Z_{22} & \cdots & Z_{2n} \\ \vdots & \vdots & \ddots & \vdots \\ Z_{n1} & Z_{n2} & \cdots & Z_{nn} \end{bmatrix} \cdot [I_i] = \begin{bmatrix} 0 \\ V_i \\ \vdots \\ 0 \end{bmatrix} \tag{3}$$

In Eq. (3), under the condition of $V_i = 1$, solving the matrix equation yields the eigen-solution $\tilde{I}_i$ when the ith cell in the array is fed individually.

$$\left[\tilde{I}_i\right] = \begin{bmatrix} Z_{11} & Z_{12} & \cdots & Z_{1n} \\ Z_{21} & Z_{22} & \cdots & Z_{2n} \\ \vdots & \vdots & \ddots & \vdots \\ Z_{n1} & Z_{n2} & \cdots & Z_{nn} \end{bmatrix}^{-1} \cdot \begin{bmatrix} 0 \\ 1 \\ \vdots \\ 0 \end{bmatrix} \tag{4}$$

It can be seen that the meaning of the array antenna eigensolution is the solution of each cell antenna individually feeding the unit amplitude voltage state. Since the matrix equation of the method of moments is linear, the solution of the method of moments under any excitation form can be obtained by the weighted linear combination of the eigensolutions as long as the eigensolutions of each cell are obtained. Equation (4) shows that the impedance matrix is invariant during the solution of the eigenvalue solution because the structure is not changed. This means that the inverse matrix of the impedance matrix needs to be solved only once. Therefore, the way of calculating the eigen-solution does not increase the computational effort significantly. For any feeder combination $(V_1, V_2, \cdots, V_n)$, the corresponding method-of-momentum solution is

$$I = \sum_{i=1}^{n} V_i \left[\tilde{I}_i\right] \tag{5}$$

The extraction of the eigensolution brings great convenience to the calculation of multi-beam antennas such as phased arrays and array feed optimization, which greatly reduces the computation time. When the radiation characteristics of the array antenna need to be optimized by adjusting the feed, the optimization algorithm only needs to update the feed amplitude and phase $(V_1, V_2, \cdots, V_n)$ to quickly combine the excitation response with feed form, and then obtain the radiation characteristics of the antenna with feed.

## 5 Radome Compensation Simulation

By modeling the antenna and the radome and using the compensation algorithm based on the eigen-solution extraction, the amplitude phase correction code values of each unit under different angles after the radome addition can be calculated. According to the simulation calculation results, the amplitude phase of each unit of phased array antenna is corrected, which can realize the optimal compensation of antenna radiation patern after radomeing.

Based on the above antenna simulation results, typical 0°, 5° and 20° angles are selected to simulate the optimized radomeed radiation patern. The typical angles such as overhead cone are selected for the azimuthal tangent of the directional diagram without radome, with radome, and after optimization as follows.

From the above simulation results, it can be seen that with beam scanning angles of 0°, 5° and 20°, for example.

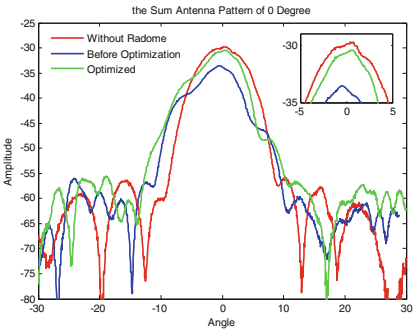


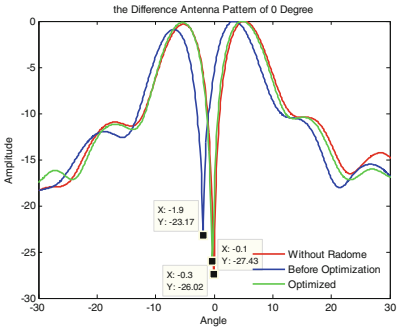


(a) The sum and Difference Antenna Pattern of 0°

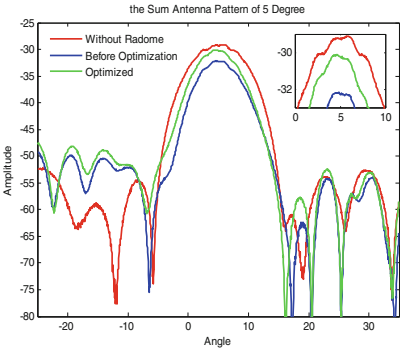


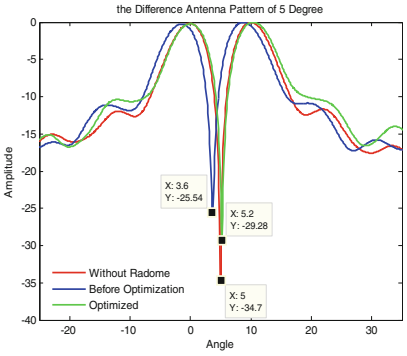


(b) The Sum and Difference Antenna Pattern of 5°

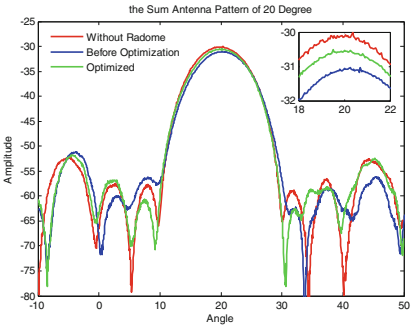


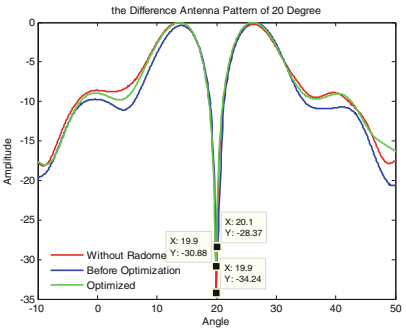


(c) The sum and Difference Antenna Pattern of 20°

**Fig. 5.** Radiation pattern of loaded radome at typical angle (compensation simulation).

After radomeing and beam gain decreased by 3.8 dB, 2.9 dB and 1 dB respectively, and the symmetry of the two main flaps of the differential beam became worse. Between 0° and 5°, the aiming line deviation is 1.5°. This is due to 0° and 5° over the top spherical part of the head cone after radomeing, due to the large difference between the cone top structure and the side wall, which has a large impact on the radiation patern loss and pointing, zero depth, etc. Then, the 20° pointing beam main flap range is not over the head cone part of the radome, and the radome side structure is uniformly symmetrical, so the impact is smaller.

After optimized compensation, the loss of 0°, 5°, 20° is 0.8 dB, 0.9 dB, 0.6 dB. Between 0° and 5°, the deviation of aiming line is optimized from 1.5° to 0.3° before compensation. After compensation, the directional loss, pointing, zero depth and other indexes of antenna are significantly optimized.

## 6 Conclusion

The introduction of the radome will bring about the deterioration of radar seeker antenna loss, pointing, aiming line error and other indexes, and there are certain limitations of the conventional structural modelling and mathematical compensation methods. In this paper, a compensation method is proposed to obtain the amplitude and phase correction values of the channel unit of the phased array seeker based on the simulation solution of the radome, which reduces the influence of the radome on the antenna performance of the seeker and ensures the working performance of the seeker under the condition of adding the radome, and the effectiveness of the method is verified by simulation.

## References

1. Priyanka, B.M., Mathur, P., Singh, H., Nair, R.U.: EM analysis of planar phased array-radome system for ground-based FCR applications. In: 2018 IEEE Indian Conference on Antennas and Propogation (InCAP), Hyderabad, India, pp. 1–2 (2018)
2. Lin, S., Lin, D., Wang, W.: A novel online estimation and compensation method for strapdown phased array seeker disturbance rejection effect using extended state kalman filter. IEEE Access **7**, 172330–172340 (2019)
3. Bui, V.P., Zhao, J., Oo, Z.Z., Sun, M., Png, C.E.: Enhanced beam scanning angle using radome design for phased array antennas. In: 2019 IEEE Asia-Pacific Microwave Conference (APMC), Singapore, pp. 1592–1594 (2019)
4. Wang, H., Zhao, Y., Huang, K., Liu, T., Gao, P.: Design of a high-performance radome for satellite communication phased array antennas. In: 2018 International Applied Computational Electromagnetics Society Symposium - China (ACES), Beijing, China, pp. 1–2 (2018)
5. Fang, C.: The calculation of quantum radar scattering characteristic for the 3d circular cone target. In: 2018 IEEE Int. Symp. Electromagn. Compat. 2018 IEEE Asia-Pacific Symp. Electromagn. Compat., pp. 248–250 (2018)
6. Fang, C.: The simulation of quantum radar scattering for 3D cylindrical targets. In: 2018 IEEE International Conference on Calculational Electromagnetics (ICCEM), Chengdu, pp. 1–3 (2018)
7. Fang, C.H.: The simulation and analysis of quantum radar cross section for 3D convex targets. IEEE Photonics J. **10**(1), 1–8 (2018)

8. Brandsema, M.J., Narayanan, R.M., Lanzagorta, M.: Theoretical and computational analysis of the quantum radar cross section for simple geometrical targets. Quantum Inf. Process. **16**(1), 1–27 (2016). https://doi.org/10.1007/s11128-016-1494-6
9. Fang, C.H., et al.: The calculation and analysis of the bistatic quantum radar cross section for the typical 2D plate. IEEE Photonics J. **10**(2), 1–14 (2018)
10. Fang, C., Han, K.: Analytical formulation for the quantum radar scattering of the rectangular plate. In: 2019 IEEE 2nd International Conference on Electronic Information and Communication Technology (ICEICT), pp. 677–681 (2019)
11. Fang, C., Shi, X.: The analysis of quantum radar scattering for the typical pyramid structure. In: 2019 IEEE International Applied Computational Electromagnetics Society Symposium in China (ACES-China) (2019)
12. Fang, C.: The analysis of mainlobeslumping quantum effect of the cube in the scattering characteristics of quantum radar. IEEE Access **7**, 141055–141061 (2019)
13. Fang, C.: The closed-form expressions for the bistatic quantum radar cross section of the typical simple plates. IEEE Sensors J. **20**(5), 2348–2355 (2020)
14. Fang, C.H., et al.: An improved physical optics method for the computation of radar cross section of electrically large objects. In: 2008 IEEE Int. Symp. Electromagn. Compat. 2008 IEEE Asia-Pacific Symp. Electromagn. Compat., pp. 722–725 (2008)